

## Quarkyonic Matter and Neutron Stars

Larry McLerran and Sanjay Reddy

*Institute for Nuclear Theory and Department of Physics, University of Washington, Seattle, Washington 98195, USA*



(Received 30 December 2018; revised manuscript received 19 February 2019; published 26 March 2019)

We consider quarkyonic matter to naturally explain the observed properties of neutron stars. We argue that such matter might exist at densities close to that of nuclear matter, and at the onset, the pressure and the sound velocity in quarkyonic matter increase rapidly. In the limit of large number of quark colors  $N_c$ , this transition is characterized by a discontinuous change in pressure as a function of baryon number density. We make a simple model of quarkyonic matter and show that generically the sound velocity is a nonmonotonic function of density—it reaches a maximum at relatively low density, decreases, and then increases again to its asymptotic value of  $1/\sqrt{3}$ .

DOI: 10.1103/PhysRevLett.122.122701

**Introduction.**—Recent radio, x-ray, and gravitational wave observations of neutron stars (NSs) have provided valuable new insights about the equation of state (EOS) of dense matter [1–3]. The discovery of two massive NSs with masses  $\simeq 2 M_\odot$  [4,5] established that the pressure of matter in the inner neutron star core, where the typical baryon number density  $n_B > 3n_0$  and  $n_0 = 0.16 \text{ fm}^{-3}$ , is large. The detection of gravitational waves from GW170817—a neutron star merger placed an upper limit on the NS tidal deformability, and provided strong evidence that their radius  $R < 13.5 \text{ km}$  [3,6–9]. These smaller radii require the pressure of matter in the outer core, where the  $n_B = 1–3n_0$ , to be relatively small. Taken together, the large observed masses and modest radii imply that the speed of sound  $c_s^2 = \partial P/\partial \epsilon$ , where  $P$  is the pressure and  $\epsilon$  is the energy density of matter, must increase rapidly in the core of the NS. Detailed analysis suggests  $c_s^2 \geq 1/3$  [10–18].

This observation that the speed of sound is of order 1 in NSs has profound consequences. The sound velocity at zero temperature can be written as

$$c_s^2 = \frac{n_B}{\mu_B d n_B / d \mu_B}, \quad (1)$$

where  $\mu_B$  is the relativistic baryonic chemical potential. This implies that when  $c_s^2 \simeq 1$ , an order 1 change of baryon density results in an order 1 change in the chemical potential. For weakly bound nuclear matter  $\mu_B \sim M_N$  this means that the chemical potential of matter must quickly increase by  $M_N$  in the neutron star core where the density changes by a factor of a few. In models that posit that nucleons are the only relevant degrees of freedom, the large change in  $\mu_B$  is achieved due to large repulsive interactions. In nonrelativistic theories  $c_s$  increases rapidly for  $n_B > n_0$  due to repulsive three-neutron interactions [19–21]. In relativistic mean field models a rapid increase in the vector potential arising due to exchange of  $\omega$  and  $\rho$  mesons shifts

the energy of nucleons by  $V_0 \simeq M_N$  [22]. Both realizations are problematic.

We now understand, through insights provided by chiral effective field theory [23,24], that nuclear Hamiltonians are only useful for  $n_B \lesssim 2n_0$  because of the proliferation of many-body operators with density [25,26]. In relativistic mean field models, large vector fields at high density shift the nucleon energy by order  $M_N$ ; here we should expect that quark degrees of freedom are important [22]. In high density quark models, there is no analog of the composite vector field to raise the zero point of the baryon energies. Recent efforts based on the functional renormalization group attempt to circumvent these problems to extend a description based only on nucleons and mesons to larger density [27]. Quarkyonic matter offers a radical alternative where both quarks and nucleons appear as quasiparticles [28,29] and provides an explicit realization of some of the early ideas concerning quark matter [30–34].

The basic assumption of quarkyonic matter is that at large Fermi energy, the degrees of freedom inside the Fermi sea may be treated as quarks, and confining forces remain important only near the Fermi surface where nucleons emerge through correlations between quarks [28]. This is somewhat analogous to the phenomena of Cooper pairing in Fermi systems with attractive interactions, where two-particle bound states smear the momentum distribution and produce an energy gap in the excitation spectrum.

In quarkyonic matter, confinement at the Fermi surface produces triplets with spin 1/2 that we identify with baryons. While we cannot offer a first-principles, QCD-based, description because we lack the nonperturbative methods needed, we provide qualitative arguments to suggest that baryons occupy a momentum shell of width  $\delta k_F = \Delta \simeq \Lambda_{\text{QCD}}$ . Because of asymptotic freedom, confining interactions arise only when the momentum exchange  $q \lesssim \Lambda_{\text{QCD}}$ . Pauli blocking of intermediate states prevents

such low-momentum exchange deep inside the quark Fermi sea and  $\Delta$  cannot be large compared to  $\Lambda_{\text{QCD}}$ . We assume that  $\Delta$  varies with density to ensure that the density of baryons in the shell saturates at  $n_B \simeq \Lambda_{\text{QCD}}^3$ , and we develop a simple model for the EOS.

The key elements of the quarkyonic picture are illustrated in Fig. 1. Here  $f_Q$  is momentum distribution function or quarks and  $E_Q$  is their energy. The momentum distribution is smeared at the surface because these quarks are confined inside baryons. Baryons occupy states near the Fermi surface with momentum width  $\Delta$  and produce a gap in the quark excitation spectrum. The absence of low energy quark excitations will have implications for the transport properties that we discuss later.

At extremely high density, quarkyonic matter is inferred from the properties of QCD when  $N_c$  is large. In this limit, confining forces are important when the Debye screening mass generated by quark loops is less than the confinement scale  $\Lambda_{\text{QCD}}$ . Since the color Debye mass  $m_D \simeq g\mu_Q$ , where  $\mu_Q$  is quark chemical potential and  $g$  is the gauge coupling, by noting that  $g^2 N_c$  is held fixed when taking the large  $N_c$  limit, we can conclude that quarks are confined into baryons for  $\mu \lesssim \sqrt{N_c} \Lambda_{\text{QCD}}$ . This observation that quark matter remains confined up to a quark chemical potential parametrically large (by the factor  $\sqrt{N_c}$ ) compared to the confinement scale is the central tenet of the quarkyonic picture [28].

To realize these ideas in a concrete example we will consider symmetric matter characterized by a finite baryon chemical potential  $\mu_B$  and the isospin chemical potential  $\mu_I = 0$ . Further, we assume that chiral symmetry remains broken to set the quark mass  $M_Q = M_N/N_c$  as in the constituent quark model, and the quark chemical potential  $\mu_Q = \mu_B/N_c$ . In the absence of interactions, nucleons will appear in the ground state when  $\mu_B > M_N$  and their number density will increase with  $\mu_B$  until the Fermi momentum  $k_{\text{FB}} \gtrsim \Lambda_{\text{QCD}}$ . Because  $M_N$  is large, at first, the nucleon

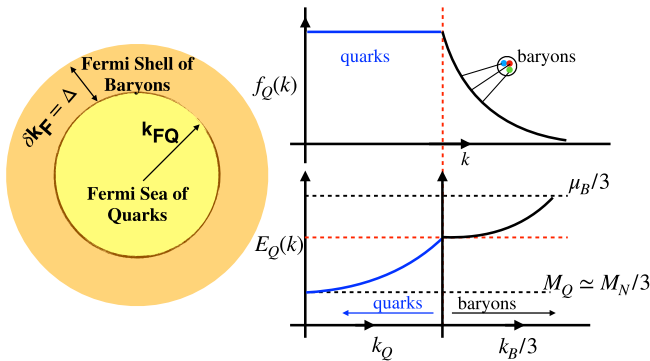


FIG. 1. The schematic shows the momentum distribution of quarks and baryons. The diffuse distribution of quarks in the right-hand upper graph indicates they are confined inside baryons that occupy momentum states with width  $\delta k_F = \Delta$ .

number density increases rapidly with  $\mu_B$ . However, when quarks appear, and occupy low-momentum states below the shell, the growth of the baryon density with  $\mu_B$  is reduced. In this model the baryon number density

$$n_B = \frac{2}{3\pi^2} [k_{\text{FB}}^3 - (k_{\text{FB}} - \Delta)^3 + k_{\text{FQ}}^3], \quad (2)$$

where  $k_{\text{FB}}$  is the Fermi momentum of nucleons, and the Fermi momentum of quarks

$$k_{\text{FQ}} = \frac{(k_{\text{FB}} - \Delta)}{N_c} \Theta(k_{\text{FB}} - \Delta), \quad (3)$$

so that the contribution of quarks to the net baryon density relative to nucleons is suppressed by  $1/N_c^3$ . The energy density is given by

$$\epsilon(n_B) = 4 \int_{N_c k_{\text{FQ}}}^{k_{\text{FB}}} \frac{d^3 k}{(2\pi)^3} \sqrt{k^2 + M_N^2} + 4N_c \int_0^{k_{\text{FQ}}} \frac{d^3 k}{(2\pi)^3} \sqrt{k^2 + M_Q^2}. \quad (4)$$

The chemical potential and pressure are obtained from the familiar thermodynamic relations  $\mu_B = \partial \epsilon / \partial n_B$  and  $P = -\epsilon + \mu_B n_B$ , respectively.

From Eq. (2) we see that  $n_B$  increases less rapidly in the quarkyonic phase. The resulting suppression of the susceptibility  $\chi_B = dn_B/d\mu_B$  leads to a rapid increase in the speed of sound and is shown as the solid blue curve in Fig. 2. The dashed blue curve shows  $c_s^2$  in noninteracting nuclear matter for density  $n_B \lesssim 3n_0$ . The black curves

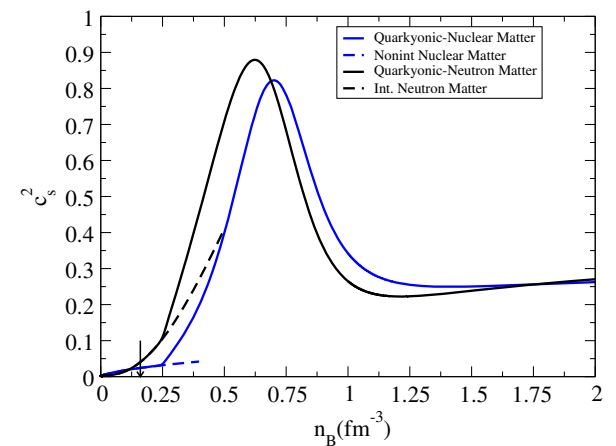


FIG. 2. The speed of sound in quarkyonic matter (solid curves) and in matter containing only nucleons (dashed curves) is shown. The blue curves are obtained for isospin symmetric nuclear matter containing equal numbers of neutron and protons, and the black curves are for matter containing only neutrons. The speed of sound at the saturation density  $n_0 = 0.16 \text{ fm}^{-3}$ , indicated by the arrow, is small and grows rapidly with increasing density.

correspond to asymmetric matter containing only neutrons and will be discussed later.

In our model we assume the thickness of quark Fermi surface where nucleons reside to be given by

$$\Delta = \frac{\Lambda^3}{k_{FB}^2} + \kappa \frac{\Lambda}{N_c^2}. \quad (5)$$

This choice is not entirely arbitrary. The first term ensures that the nucleon density  $n_N \propto k_{FB}^2 \Delta \approx \Lambda^3$  approximately saturates when baryons dominate the energy density. We can expect such behavior when many-body interactions between nucleons are repulsive and lead to a rapid increase in the energy per baryon with density. The second term is needed to ensure that  $c_s^2 < 1$ . We set  $N_c = 3$ ,  $\Lambda = 300$  MeV, and  $\kappa = 0.3$  to obtain the results shown in Fig. 2. Quarkyonic matter generically predicts a rapid increase in the sound velocity for  $k_{FB} \gtrsim \Lambda$ , but its evolution with density depends sensitively on the details. For our *Ansätze* the location of the maximum of  $c_s$  is largely determined by  $\Lambda$  and its magnitude depends on both  $\Lambda$  and  $\kappa$ .

The transition from nuclear matter to the quarkyonic phase is second order in our simple model. The speed of sound is continuous, but its derivative is not. As quarks appear, pressure remains a smooth, but a more rapidly increasing function of the energy density. This is the opposite of the behavior encountered in simple models of the quark-hadron transition, where the transition from nuclear matter to quark matter leads to a reduction in the pressure. Such transitions are typically first order and soften the EOS even in the presence of a mixed phase containing spatially separated quark and hadronic phases[35].

Thus far we have neglected nuclear interactions. At low density, attractive nuclear interactions bind nucleons in nuclei, and uniform symmetric nuclear matter is stable at higher density due to repulsive hard-core interactions. In nuclear models the speed of sound increases largely due to these hard-core interactions. In contrast, since the nucleon density in the quarkyonic phase saturates at  $n_B \propto \Lambda_{QCD}^3$ , nuclear interactions do not change the qualitative behavior seen in Fig. 2. However, nuclear interactions are quantitatively important and will be relevant in the following when we discuss the EOS of neutron matter in the context of neutron stars.

To describe neutron star matter we need to impose local charge neutrality and beta equilibrium. These constraints restrict the proton fraction to be  $\lesssim 10\%$ . For this reason, we will approximate matter to consist of only neutrons. At a given baryon density  $n_B$ , the neutron Fermi momenta is denoted by  $k_{FB}$  and the up and down quark Fermi momenta are denoted by  $k_{Fu}$  and  $k_{Fd}$ , respectively. We set  $k_{Fd} = (k_{FB} - \Delta)/3$  for  $k_{FB} > \Delta$  and  $k_{Fu} = k_{Fd}/2^{1/3}$  to ensure charge neutrality.

Calculations of the EOS of neutron matter and their use in constructing neutron stars have established the importance of interactions between neutrons. When the neutron density  $n_n \lesssim n_0$ , interactions are predominantly attractive, and act to reduce the pressure of the neutron matter. With increasing density, repulsive two- and three-body interactions between neutrons at short distances become important and lead to a rapid increase in the pressure [19,20,36]. This transition plays an important role in determining the radius of NSs with mass  $M \simeq 1.4 M_\odot$  [37]. To incorporate interactions we adopt a simple fit to microscopic calculations of neutron matter from Ref. [38], where the energy density due to interactions for  $n_n < 2n_0$  was well approximated by

$$V_n(n_n) = \tilde{a} n_n \left( \frac{n_n}{n_0} \right) + \tilde{b} n_n \left( \frac{n_n}{n_0} \right)^2. \quad (6)$$

Here the coefficients  $\tilde{a} = -28.6 \pm 1.2$  MeV and  $\tilde{b} = 9.9 \pm 3.7$  MeV are chosen to bracket the uncertainties due to poorly constrained three-neutron forces [20,21]. Further, making the assumption that the interaction energy of neutrons in the shell is only a function of the number density of neutrons in the shell,

$$n_n = \frac{k_{FB}^3 - (k_{FB} - \Delta)^3}{3\pi^2}, \quad (7)$$

the energy density of quarkyonic matter is

$$\epsilon(n_B) = 2 \int_{k_{FB}-\Delta}^{k_{FB}} \frac{d^3 k}{(2\pi)^3} \sqrt{k^2 + M_N^2} + V_n(n_n) + 2 \sum_{i=u,d} N_c \int_0^{k_{Fi}} \frac{d^3 k}{(2\pi)^3} \sqrt{k^2 + M_Q^2}, \quad (8)$$

and the total baryon density is

$$n_B = n_n + \frac{(k_{Fd}^3 + k_{Fu}^3)}{3\pi^2}. \quad (9)$$

The chemical potential and pressure are  $\mu_B = (\partial \epsilon / \partial n_B)$  and  $P = -\epsilon + \mu_B n_B$ , respectively.

In Fig. 2, the solid black curve shows  $c_s^2$  in quarkyonic-neutron matter. Here we include the interaction contribution between neutrons in the shell.  $c_s^2$  in pure neutron matter is also shown as the black dotted curve for  $n_B \lesssim 3n_0$ . The interaction energy is obtained by setting  $\tilde{a} = -28.8$  MeV and  $\tilde{b} = 10.0$  MeV and corresponds to a symmetry energy of 32 MeV and the pressure  $P(n_0) = 2.4$  MeV/fm<sup>3</sup> and is compatible with experimental constraints [39]. The kinetic contribution of the quarks in the sea and nucleons in the shell is included as discussed earlier.  $\Delta$  is given by Eq. (5) and we set  $\Lambda = 380$  MeV and  $\kappa = 0.3$ . With this choice

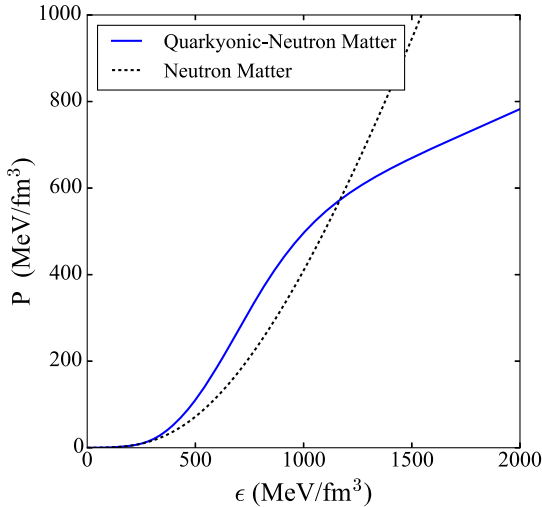


FIG. 3. EOS of quarkyonic matter and neutron matter. The model is discussed in the text.

quarkyonic matter occurs at  $n_B = 0.24 \text{ fm}^{-3}$  and the maximum value of  $c_s \simeq 0.94$  is reached at  $n_B = 0.64 \text{ fm}^{-3}$ .

The EOS of quarkyonic-neutron matter is shown (solid blue curve) in Fig. 3 for the model parameters mentioned above. The EOS of neutron matter without quarks obtained by setting  $k_{FQ} = 0$  is also shown. The rapid increase in pressure at the onset of the quarkyonic phase is remarkable and its influence on the neutron star mass-radius curve is shown in Fig. 4. For comparison the mass-radius curve for pure neutron matter is also shown. Since quarkyonic matter

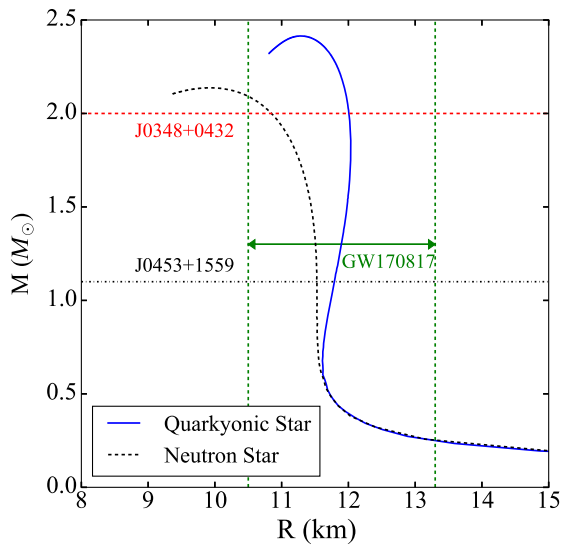


FIG. 4. Mass-radius curve of a quarkyonic star (solid curve) is compared to that of an ordinary neutron star. The EOS in the core is described in the text and the EOS of the outer and inner crust are taken from Refs. [40,41], respectively. The largest and smallest observed neutron star masses, and the limits on the radii of the neutron stars inferred from the observation of gravitational waves from GW170817, are also shown.

has larger pressure over a range of energy densities encountered in the core, it is able to support a larger maximum mass and predicts radii that are also a bit larger. Uncertainty associated with neutron matter and the quarkyonic matter EOSs are presently too large to make discernible predictions for neutron star masses and radii. Our proposal offers an alternate scenario for the rapid increase in the pressure, which does not rely on large contributions from nuclear interactions. Further, since low energy excitations near the Fermi surface are baryonic, we can expect transport properties including neutrino cooling of quarkyonic matter to be quite similar to those encountered in nuclear matter. However, more work is warranted to determine if there could be discernible differences, and how one would access it observationally.

A model in which interactions between quarks generate baryons at the Fermi surface would provide useful insights about quarkyonic matter. In future work such models could be obtained by generalizing Nambu–Jona-Lasinio models used to study color superconductivity [42,43]. Here Cooper pairs favored in weak coupling would be replaced by baryons due to strong confining interactions between three quarks at the Fermi surface [44]. Related ideas on the interplay between quarks, diquarks, and baryons have been suggested and explored in earlier work (see, e.g., Refs. [45,46]) but differ from our proposal.

L. M. gratefully acknowledges useful conversations with Jean Paul Blaizot, Volker Koch, and Toru Kojo. S. R. gratefully acknowledges conversations with members of the N3AS Collaboration. L. M. and S. R. thank Chuck Horowitz for comments on the manuscript and useful conversations. The work of L. M. and S. R. was supported by the U.S. DOE under Grant No. DE-FG02-00ER41132.

- [1] A. L. Watts, N. Andersson, D. Chakrabarty, M. Feroci, K. Hebeler, G. Israel, F. K. Lamb, M. C. Miller, S. Morsink, F. Özel, A. Patruno, J. Poutanen, D. Psaltis, A. Schwenk, A. W. Steiner, L. Stella, L. Tolos, and M. van der Klis, *Rev. Mod. Phys.* **88**, 021001 (2016).
- [2] F. Özel and P. Freire, *Annu. Rev. Astron. Astrophys.* **54**, 401 (2016).
- [3] B. P. Abbott *et al.* (LIGO Scientific Collaboration and Virgo Collaboration), *Phys. Rev. Lett.* **121**, 161101 (2018).
- [4] P. Demorest, T. Pennucci, S. Ransom, M. Roberts, and J. Hessels, *Nature (London)* **467**, 1081 (2010).
- [5] J. Antoniadis *et al.*, *Science* **340**, 1233232 (2013).
- [6] E. Annala, T. Gorda, A. Kurkela, and A. Vuorinen, *Phys. Rev. Lett.* **120**, 172703 (2018).
- [7] A. Vuorinen, *Nucl. Phys.* **A982**, 36 (2019).
- [8] S. De, D. Finstad, J. M. Lattimer, D. A. Brown, E. Berger, and C. M. Biwer, *Phys. Rev. Lett.* **121**, 091102 (2018).
- [9] I. Tews, J. Margueron, and S. Reddy, *Phys. Rev. C* **98**, 045804 (2018).
- [10] M. Alford, M. Braby, M. W. Paris, and S. Reddy, *Astrophys. J.* **629**, 969 (2005).

[11] N. Chamel, A. F. Fantina, J. M. Pearson, and S. Goriely, *Astron. Astrophys.* **553**, A22 (2013).

[12] K. Masuda, T. Hatsuda, and T. Takatsuka, *Prog. Theor. Exp. Phys.* (2013), 073D01.

[13] M. G. Alford, S. Han, and M. Prakash, *Phys. Rev. D* **88**, 083013 (2013).

[14] T. Kojo, P. D. Powell, Y. Song, and G. Baym, *Phys. Rev. D* **91**, 045003 (2015).

[15] P. Bedaque and A. W. Steiner, *Phys. Rev. Lett.* **114**, 031103 (2015).

[16] I. Tews, J. Carlson, S. Gandolfi, and S. Reddy, *Astrophys. J.* **860**, 149 (2018).

[17] Y.-L. Ma and M. Rho, [arXiv:1811.07071](https://arxiv.org/abs/1811.07071).

[18] S. K. Greif, G. Raaijmakers, K. Hebeler, A. Schwenk, and A. L. Watts, [arXiv:1812.08188](https://arxiv.org/abs/1812.08188).

[19] A. Akmal, V. R. Pandharipande, and D. G. Ravenhall, *Phys. Rev. C* **58**, 1804 (1998).

[20] K. Hebeler and A. Schwenk, *Phys. Rev. C* **82**, 014314 (2010).

[21] S. Gandolfi, J. Carlson, and S. Reddy, *Phys. Rev. C* **85**, 032801 (2012).

[22] B. D. Serot and J. D. Walecka, *Int. J. Mod. Phys. E* **06**, 515 (1997).

[23] S. Weinberg, *Phys. Lett. B* **251**, 288 (1990).

[24] D. B. Kaplan, M. J. Savage, and M. B. Wise, *Phys. Lett. B* **424**, 390 (1998).

[25] U. van Kolck, *Phys. Rev. C* **49**, 2932 (1994).

[26] E. Epelbaum, H.-W. Hammer, and Ulf-G. Meissner, *Rev. Mod. Phys.* **81**, 1773 (2009).

[27] M. Drews and W. Weise, *Prog. Part. Nucl. Phys.* **93**, 69 (2017).

[28] L. McLerran and R. D. Pisarski, *Nucl. Phys.* **A796**, 83 (2007).

[29] Y. Hidaka, L. D. McLerran, and R. D. Pisarski, *Nucl. Phys. A* **808**, 117 (2008).

[30] N. Itoh, *Prog. Theor. Phys.* **44**, 291 (1970).

[31] J. C. Collins and M. J. Perry, *Phys. Rev. Lett.* **34**, 1353 (1975).

[32] G. Baym and S. Chin, *Phys. Lett.* **62B**, 241 (1976).

[33] B. Freedman and L. D. McLerran, *Phys. Rev. D* **17**, 1109 (1978).

[34] G. Baym, *Physica (Amsterdam)* **96A**, 131 (1979).

[35] N. K. Glendenning, *Phys. Rev. D* **46**, 1274 (1992).

[36] S. Gandolfi, A. Yu. Illarionov, K. E. Schmidt, F. Pederiva, and S. Fantoni, *Phys. Rev. C* **79**, 054005 (2009).

[37] J. M. Lattimer and M. Prakash, *Science* **304**, 536 (2004).

[38] S. Gandolfi, J. Carlson, S. Reddy, A. W. Steiner, and R. B. Wiringa, *Eur. Phys. J. A* **50**, 10 (2014).

[39] M. B. Tsang, J. R. Stone, F. Camera, P. Danielewicz, S. Gandolfi, K. Hebeler, C. J. Horowitz, J. Lee, W. G. Lynch, Z. Kohley, R. Lemmon, P. Möller, T. Murakami, S. Riordan, X. Roca-Maza, F. Sammarruca, A. W. Steiner, I. Vidaña, and S. J. Yennello, *Phys. Rev. C* **86**, 015803 (2012).

[40] G. Baym, C. Pethick, and P. Sutherland, *Astrophys. J.* **170**, 299 (1971).

[41] J. W. Negele and D. Vautherin, *Nucl. Phys.* **A207**, 298 (1973).

[42] M. G. Alford, K. Rajagopal, and F. Wilczek, *Phys. Lett. B* **422**, 247 (1998).

[43] M. Buballa, *Phys. Rep.* **407**, 205 (2005).

[44] M. G. Alford, A. Schmitt, K. Rajagopal, and T. Schäfer, *Rev. Mod. Phys.* **80**, 1455 (2008).

[45] K. Fukushima and T. Kojo, *Astrophys. J.* **817**, 180 (2016).

[46] G. Baym, T. Hatsuda, T. Kojo, P. D. Powell, Y. Song, and T. Takatsuka, *Rep. Prog. Phys.* **81**, 056902 (2018).